Analysis of Sparse and Noisy Ocean Current Data Using Flow Decomposition. Part I: Theory

PETER C. CHU AND LEONID M. IVANOV

Naval Postgraduate School, Monterey, California

TATIANA P. KORZHOVA, TATIANA M. MARGOLINA, AND OLEG V. MELNICHENKO

Marine Hydrophysical Institute and Center for Ecological Modeling and Recreation Geography, National Ukrainian Academy of Sciences, Sevastopol, Crimea, Ukraine

(Manuscript received 5 November 2001, in final form 9 September 2002)

ABSTRACT

A new approach is developed to reconstruct a three-dimensional incompressible flow from noisy data in an open domain using a two-scalar (toroidal and poloidal) spectral representation. The results are presented in two parts: theory (first part) and application (second part). In Part I, this approach includes (a) a boundary extension method to determine normal and tangential velocities at an open boundary, (b) establishment of homogeneous open boundary conditions for the two potentials with a spatially varying coefficient κ, (c) spectral expansion of κ, (d) calculation of basis functions for each of the scalar potentials, and (e) determination of coefficients in the spectral decomposition of both velocity and κ using linear or nonlinear regressions. The basis functions are the eigenfunctions of the Laplacian operator with homogeneous mixed boundary conditions and depend upon the spatially varying parameter κ at the open boundary. A cost function used for poor data statistics is introduced to determine the optimal number of basis functions. An optimization scheme with iteration and regularization is proposed to obtain unique and stable solutions. In Part II, the capability of the method is demonstrated through reconstructing a 2D wind-driven circulation in a rotating channel, a baroclinic circulation in the eastern Black Sea, and a large-scale surface circulation in the Southern Ocean.

1. Introduction

Ocean observational current data are usually acquired from limited number of stations in domains with open boundaries and contain various errors or noises. It is an important task for physical oceanographers to establish (or to reconstruct) a realistic and complete velocity field from sparse and noisy data.

From a mathematical point of view, the reconstruction requires solving a least square problem without or with a priori information (limit) on the circulation characteristics. An a priori limit can be formulated as a set of inequalities that the solutions should satisfy, as a dynamical model applied to the description of circulation dynamics or hypotheses on statistical properties of reconstructed field.

Several techniques are available for fulfilling such a task: various kinds of spline interpolation (e.g., Washba and Wendelberger 1980; Smith and Wessel 1990; Brankart and Brasseur 1996), optimal interpolation (OI; e.g., Gandin 1965), fitting models (Cho et al. 1998; Lipphardt et al. 1977, 2000), objective mapping combined with a fitting (e.g., Davis 1985), and numerous approaches using ocean numerical models such as the adjoint method and Kalman filter (e.g., Malonette-Rizzoli and Tziperman 1996).

Several error sources deteriorate the reconstruction skill. One of them is the uncertainty in boundary conditions, especially at open boundaries. Therefore, how to determine open boundary conditions becomes a key issue in the reconstruction process.

The classical OI technique does not allow accounting for any boundary condition as an a priori limitation. Davis (1985) used a combined OI–spectral fitting model with a priori knowledge of the statistical weights to overcome this weakness. However, it remains uncertain how to select the weights for an open domain and how to determine basis functions with a priori nonzero flux at the open boundary.

With velocities given along the open boundary and with an additional boundary condition such as the "natural" boundary condition (Courant and Hilbert 1966), the spline functions can be used as universal basis functions. However, a detailed analysis (Inoue 1986) shows

Corresponding author address: Dr. Peter C. Chu, Naval Ocean Analysis and Prediction Lab, Department of Oceanography, Naval Postgraduate School, Monterey, CA 93943.
E-mail: chu@nps.navy.mil

© 2003 American Meteorological Society

that the natural boundary condition is more appropriate for rigid than open boundaries.

An effective approach to determine open boundary condition is to use an optimization procedure together with an ocean numerical model such as the adjoint method (e.g., Seiler 1993), the Jacobian matrix method (e.g., Chu et al. 1997), and the local variation principle (e.g., Shulman and Lewis 1995). The open boundary conditions can be determined through minimizing the difference between observations and model estimations inside the integration domain. These approaches need to solve an ill-posed inverse problem using an iteration procedure independent of the chosen local boundary conditions. To ensure their convergence to physical reality, we need a "good" initial approximation for the open boundary conditions even if the noise-to-signal ratio in the data is small (Engl et al. 1996).

Without knowing statistical weights and without using ocean numerical models, a kinematical method is proposed for reconstructing a velocity field from noisy and sparse data. For a three-dimensional incompressible flow, two scalar functions, toroidal (Ψ) and poloidal (Φ) potentials, satisfy Poisson equations with the vertical vorticity ($\zeta = \partial v/\partial x - \partial u/\partial y$) and vertical velocity (w) as the sources terms, respectively (Moffat 1978; Eremeev et al. 1992a,b; Chu 1999; Chu et al. 2002).

The two potentials (Φ, Ψ) are expanded into a series of basis functions, which are eigenfunctions of the Laplacian operator for the given geometry of the ocean domain and homogeneous boundary conditions. For a closed basin with no slip on the rigid boundary, it is typical to use the Dirichlet and Neumann boundary conditions for Ψ and Φ (Eremeev et al. 1992a,b), and to use the Dirichlet boundary condition for the transport streamfunction (Rao and Schwab 1981). This procedure allowed construction of basis functions and reconstruction of the velocity field from data for the Black Sea (Eremeev et al. 1992a,b) and Lake Ontario (Rao and Schwab 1981), both treated as closed basins.

Lipphardt et al. (2000) proposed an approach for a domain with an open boundary through expanding the poloidal potential into a combination of harmonic functions satisfying boundary conditions a priori given from a large-scale numerical model and a spectral decomposition with the basis functions as the eigenfunctions of the Laplacian operator with homogeneous Neumann conditions. The reconstruction skill of their method strongly depends on the quality of the numerical model.

In this study, a new set of basis functions is introduced for reconstructing the ocean circulation in a domain with open boundaries. These functions are the eigenfunctions of the Laplacian operator with homogeneous mixed conditions. With known velocities along the open boundary, the mixed boundary conditions are accurate. With unknown velocities along the open boundary, a parameterization scheme is proposed for obtaining approximate open boundary conditions from data. In general, the reconstruction is reduced to linear and nonlinear regression models for known and unknown velocities along the open boundary, respectively. For the latter (without data on the open boundary), the velocity inside the domain and along the boundaries are simultaneously determined.

The reconstruction skill depends on various factors such as the noise level in the data, the sampling strategy, and the quality of numerical algorithms used in the reconstruction. This study shows that even if the combination of all the factors is not favorable, the reconstructed circulation pattern and the velocity along the open boundary are acceptable according the criterion mentioned in the text. Thus, the proposed reconstruction scheme is a useful tool in analyzing kinematic and energetic characteristics of the circulation, and provides zero-order initial conditions for numerical ocean models.

The outline of this paper is as follows. In section 2, we describe the decomposition of flow into poloidal and toroidal components, specify the boundary conditions for both potentials, and introduce two sets of complete basis functions. In section 3, we depict the principal relationships used in the reconstruction process. In section 4, we discuss a regularization technique. In section 5, we provide an approach to determine the optimal number of basis functions used in linear or nonlinear regression models, and two criteria such as Vapnik–Chervonkis cost function, and root-mean-square errors to determine the reconstruction skill. In section 6, we give conclusions.

2. Two scalar potentials

a. Toroidal and poloidal components

In magnetohydrodynamics and astrophysics, it is common to decompose any vector $\mathbf{Q}$ in an arbitrary coordinate system into three parts (Dubrovin et al. 1992). For example, it is in spherical coordinate system, written as

$$\mathbf{Q} = \mathbf{r} \times \nabla A_1 + \mathbf{r} A_2 + \nabla A_3, \tag{2.1}$$

where A_1, A_2, and A_3 are scalar functions (see appendix A), ∇ is the three-dimensional gradient operator, and $\mathbf{r}$ is the radius vector from the origin. Borrowing this idea for ocean currents ($\mathbf{Q} = \mathbf{u}$) satisfying the incompressible property

$$\nabla \cdot \mathbf{u} = 0, \tag{2.2}$$

the three-dimensional velocity field at large-, meso-, and submesoscales is represented by [(A.5), see appendix A]:

$$\mathbf{u} = \nabla \times (\mathbf{r}\Psi) + \nabla \times \nabla \times (\mathbf{r}\Phi), \tag{2.3}$$

where the two terms in the right-hand side of (2.3) are called toroidal and poloidal velocities.

If the velocity is reconstructed on horizontal planes, the radius vector $\mathbf{r}$ can be replaced by the unit vector

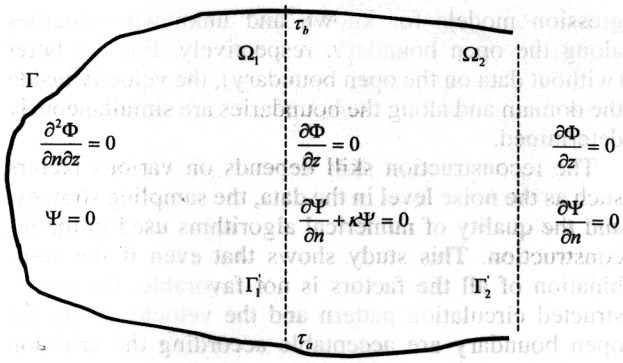

FIG. 1. Boundary conditions and open boundary extension method.

in the vertical direction **k** (Moffat 1978). Thus, the velocity **u** (u, v, w), determined on any horizontal plane, is represented by (Eremeev et al. 1992a,b)

$$u = \frac{\partial\Psi}{\partial y} + \frac{\partial^2\Phi}{\partial x\partial z}, \quad v = -\frac{\partial\Psi}{\partial x} + \frac{\partial^2\Phi}{\partial y\partial z}, \quad \text{and}$$
$$w = -\Delta\Phi, \tag{2.4}$$

where the Cartesian coordinate system is used with (x, y) and z as the horizontal and vertical coordinates, respectively.

Obviously, both toroidal and poloidal potentials satisfy the Poisson equations

$$\Delta\Psi = -\zeta \quad \text{and} \tag{2.5a}$$
$$\Delta\Phi = -w. \tag{2.5b}$$

Here, $\Delta \equiv \partial^2/\partial x^2 + \partial^2/\partial y^2$ is the two-dimensional Laplacian operator, and $\zeta = \partial v/\partial x - \partial u/\partial y$ is the vertical component of vorticity.

In general, the toroidal and poloidal potentials Ψ and Φ are not the same as the geostrophic stream function and velocity potential commonly used in meteorology and oceanography (e.g., Lynch 1988). If the Coriolis parameter varies considerably within the domain, the poloidal potential satisfies the Poisson equation with a source term determined by the horizontal velocity and the gradient of the Coriolis parameter even in the pure geostrophic flow. That can be checked out through the direct substitution of (2.4) into the geostrophic equations.

Before introducing a new set of basis functions for an open domain, one should answer the question, What boundary conditions will be used for toroidal and poloidal potentials? Let fluid be in a simply connected domain with rigid (Γ) and open (Γ_1') boundaries. The open boundary has two end points τ_a and τ_b (Fig. 1). Both toroidal and poloidal potentials satisfy Poisson equations with coupled boundary conditions. Along the boundary, the velocity is decomposed into normal (V_n) and tangential (V_τ) components

$$V_n = \frac{\partial\Psi}{\partial\tau} + \frac{\partial^2\Phi}{\partial n\partial z}, \qquad V_\tau = -\frac{\partial\Psi}{\partial n} + \frac{\partial^2\Phi}{\partial\tau\partial z}, \tag{2.6}$$

where (n, τ) represent normal and tangential unit vectors along $\Gamma \cup \Gamma_1'$.

b. Rigid boundary segment (Γ)

Along the rigid boundary (Γ) segment, the kinematic boundary conditions are given by

$$V_n = 0, \qquad V_\tau \neq 0.$$

The two scalar potentials satisfy (Eremeev et al. 1992a,b)

$$\Psi|_\Gamma = C, \qquad \left.\frac{\partial^2\Phi}{\partial n\partial z}\right|_\Gamma = 0, \tag{2.7}$$

where C is a constant to be determined. Since τ_a and τ_b are also the two end points of the rigid segment, we have

$$\Psi|_{\tau_a} = \Psi|_{\tau_b} = C.$$

Note that the scalar potentials Ψ and Φ cannot be determined if the velocity at the rigid segment vanishes (Ladyzhenskaya 1969):

$$V_n = V_\tau = 0.$$

c. Open boundary segment (Γ_1')

When the normal (V_n) and tangential (V_τ) components are given, we integrate the first equation in (2.6) with respect to τ along the open boundary segment (Γ_1') from the end point τ_a,

$$\Psi(\tau) = \Psi|_{\tau_a} + \int_{\tau_a}^{\tau}\left(V_n - \frac{\partial^2\Phi}{\partial n\partial z}\right)d\tau', \tag{2.8}$$

and define a coefficient $\kappa(\tau)$ varying along Γ_1' by

$$\kappa(\tau) = \frac{-\left(V_\tau - \dfrac{\partial^2\Phi}{\partial\tau\partial z}\right)}{\displaystyle\int_{\tau_a}^{\tau}\left(V_n - \frac{\partial^2\Phi}{\partial n\partial z}\right)d\tau' + C}. \tag{2.9}$$

The boundary condition for Ψ is obtained from (2.6):

$$\left[\frac{\partial\Psi}{\partial n} + \kappa(\tau)\Psi\right]\Bigg|_{\Gamma_1'} = 0, \tag{2.10}$$

where $\tau \in [\tau_a, \tau_b]$, is a moving point along Γ_1'.

When the constant C in (2.9) vanishes, the coefficient $\kappa(\tau)$ tends to infinity as τ tends to τ_a or τ_b. From the theoretical point of view, such a behavior of $\kappa(\tau)$ does not add any complexity in applying (2.10). First, the singularity of $\kappa(\tau)$ can be effectively eliminated by a perturbation technique (Morse and Freshbach 1953) due to the toroidal potential Ψ being a smooth function along the boundary Γ_1'. Second, we may transform (2.10) into

$$\left[\kappa_1(\tau)\frac{\partial\Psi}{\partial n} + \kappa_2(\tau)\Psi\right]\Big|_{\Gamma_1'} = 0,$$

where no singularity occurs. Here

$$\kappa_1(\tau) = \int_{\tau_a}^{\tau}\left(V_n - \frac{\partial^2\Phi}{\partial n\partial z}\right)d\tau' + C,$$

$$\kappa_2(\tau) = -\left(V_\tau - \frac{\partial^2\Phi}{\partial\tau\partial z}\right).$$

In this paper, these conditions are not used because the unknown open boundary condition is assumed a priori. A smooth function is used to parameterize $\kappa(\tau)$ and in turn to provide an approximate open boundary condition.

d. Basis functions

1) SIMPLY CONNECTED ENCLOSED DOMAIN

For a domain with an enclosed rigid boundary (Γ), the appropriate basis functions $\{\Psi_k\}$ and $\{\Phi_m\}$ are given by

$$\Delta\Psi_k = -\lambda_k\Psi_k, \qquad \Psi_k|_\Gamma = 0, \qquad k = 1, \ldots, \infty, \tag{2.11}$$

$$\Delta\Phi_m = -\mu_m\Phi_m, \quad \frac{\partial\Phi_m}{\partial n}\Big|_\Gamma = 0, \qquad m = 1, \ldots, \infty. \tag{2.12}$$

Here, $\{\lambda_k\}$ and $\{\mu_m\}$ are the corresponding eigenvalues. Similar basis functions were obtained by Rao and Schwab (1981) for Lake Ontario, and Eremeev et al. (1992a,b) for the Black Sea, respectively.

2) SIMPLY CONNECTED OPEN DOMAIN

Both velocity components (V_n, V_τ) are usually nonzero at the open boundary Γ_1'. The toroidal potential Ψ satisfies the boundary condition (2.10) with the parameter $\kappa(\tau)$ depending on Φ. Thus, a possible approach is to specify Φ at the open boundary to obtain a condition for Ψ.

(i) Minimum poloidal kinetic energy assumption

Decomposition of the velocity field into toroidal and poloidal parts can take various forms. The potentials have no physical significance themselves (Ladyzhenskaya 1969). They are meaningful only in representing the circulation. To reduce the degree of freedom without loss of any generality, the poloidal kinetic energy is assumed averaged over the domain including the open boundary to be minimal and obtain, according to Pedersen (1971),

$$\frac{\partial\Phi}{\partial z} = 0 \quad \text{at } \Gamma_1'. \tag{2.13}$$

Thus, the boundary conditions for the rigid and open segments are represented by (2.7) and (2.10), (2.13), respectively. The corresponding basis functions are the eigenfunctions of the following spectral problems:

$$\Delta\Psi_k = -\lambda_k\Psi_k, \tag{2.14}$$

$$\Delta\Phi_m = -\mu_m\Phi_m, \tag{2.15}$$

$$\Psi_k|_\Gamma = 0, \quad \frac{\partial\Phi_m}{\partial n}\Big|_\Gamma = 0, \quad \text{and} \tag{2.16}$$

$$\left[\frac{\partial\Psi_k}{\partial n} + \kappa(\tau)\Psi_k\right]\Big|_{\Gamma_1'} = 0, \qquad \Phi_m|_{\Gamma_1'} = 0, \tag{2.17}$$

which are the mixed boundary conditions formulated for a simply connected domains.

(ii) Features of the basis functions

The basis functions defined by (2.14)–(2.17) have the following features.

1) Each of the two sets of basis functions $\{\Psi_k\}$ and $\{\Phi_m\}$ is orthonormal and complete (Vladimirov 1971). To calculate directly these basis functions, it requires a priori knowledge of geometry and velocity components at the boundary (i.e., a known boundary condition). For unknown boundary conditions, a nonlinear regression scheme should be developed.
2) Three reasons make the basis functions defined here more appropriate than trigonometric polynomials (plane geometry) and spherical harmonics (spherical geometry) in flow reconstruction from noisy and sparse data. First, the trigonometric polynomials and spherical harmonics are not the solutions of (2.14)–(2.17) for a domain with complex boundaries and/or with κ varying along the open boundary. That is to say that the trigonometric polynomials and spherical harmonics cannot formulate a complete set of basis functions in this case. Second, the spectral series usually converges quicker using the basis functions determined by (2.14)–(2.17) than using trigonometric polynomials and spherical harmonics since the physical information at the boundary is sufficiently used. This leads to fewer modes needed using $\{\Psi_k\}$ and $\{\Phi_m\}$ as the basis functions than using the trigonometric polynomials and spherical harmonics.
3) If normal and tangential velocities along the open boundary change with time, the coefficient κ also depends on time. The velocity field should be reconstructed at a particular time. This usually does not add any complexity to the reconstruction. However, it may consume considerable computer resources if (2.9) is applied for the analysis of long-term observation series. This topic will not be discussed further in this paper.
4) The boundary condition (2.10) may be simplified, for example, assuming zero tangential velocity at an

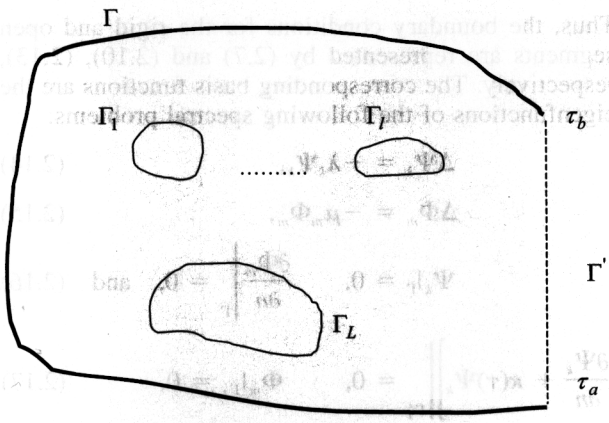

FIG. 2. A multiply connected domain.

extended open boundary Γ_2'. The boundary conditions become (Fig. 1)

$$\left.\frac{\partial \Psi}{\partial n}\right|_{\Gamma_2'} = 0, \qquad \left.\frac{\partial \Phi}{\partial z}\right|_{\Gamma_2'} = 0. \tag{2.18}$$

The solutions of (2.14) and (2.15) are relatively easy to obtain since $\{\Psi_k\}$ and $\{\Phi_m\}$ do not depend on each other. Notice that the condition (2.18) allows for nonzero normal velocity along the open boundary.

5) The approach can be extended to a multiply connected domain through the methodology originally described by Kamenkovich (1961). This is demonstrated through circulation reconstruction in the Southern Ocean from the drifter data [see Part II, (Chu et al. 2003)].

3) MULTIPLY CONNECTED OPEN DOMAIN

Consider a multiply connected domain with a rigid boundary Γ and an open boundary Γ'. Inside the domain, there are L islands with rigid boundaries $\Gamma_1, \Gamma_2 \ldots, \Gamma_L$ (Fig. 2). The solution of the Poisson equation (2.5a) can be decomposed into (Vladimirov 1971):

$$\Psi = \sum_{l=1}^{L} C_l \hat{\Psi}^{(l)} + C\hat{\Psi} + \tilde{\Psi}, \tag{2.19}$$

such that the harmonic functions $\hat{\Psi}^{(l)}$ and $\hat{\Psi}$ satisfy the Laplacian equation

$$\Delta\hat{\Psi}^{(l)} = 0, \qquad \Delta\hat{\Psi} = 0, \tag{2.20}$$

with the inhomogeneous boundary condition

$$\hat{\Psi}^{(l)} = \begin{cases} 1 & \text{on } \Gamma_l \\ 0 & \text{on } \Gamma, \Gamma', \text{ and } \Gamma_{l'}(l' \neq l), \end{cases}$$

$$\hat{\Psi} = \begin{cases} 1 & \text{on } \Gamma \cup \Gamma' \\ 0 & \text{on } \Gamma_l \quad (l = 1, 2, \ldots, L). \end{cases} \tag{2.21}$$

Here, $C_l (l = 1, 2, \ldots, L)$ and C are the integration constants along the boundaries $\Gamma_1, \Gamma_2, \ldots, \Gamma_L$, and $\Gamma \cup \Gamma'$.

The variable $\tilde{\Psi}$ satisfies

$$\Delta\tilde{\Psi} = -\zeta \tag{2.22}$$

with the homogeneous boundary conditions,

$$\tilde{\Psi}|_{\Gamma_1,\Gamma_2,\ldots,\Gamma_L,\Gamma} = 0, \qquad \left[\frac{\partial\tilde{\Psi}}{\partial n} + \kappa\tilde{\Psi}\right]\Bigg|_{\Gamma'} = 0. \tag{2.23}$$

where the coefficient κ is given by

$$\kappa = \frac{-\left(V_\tau - \dfrac{\partial^2\Phi}{\partial\tau\partial z} - C\dfrac{\partial\tilde{\Psi}}{\partial n}\right)}{\displaystyle\int_{\tau_a}^{\tau}\left(V_n - \frac{\partial\Phi}{\partial n\partial z}\right)d\tau'}. \tag{2.24}$$

The $(L + 1)$ constants, $C_l (l = 1, 2, \ldots, L)$ and C should be determined by the data or by additional dynamic constraints (Kamenkovich 1961; McWilliams 1977; Flierl 1977).

The poloidal potential satisfies

$$\Delta\Phi = -w,$$

with the rigid boundary conditions

$$\frac{\partial\Phi}{\partial z\partial n} = 0 \quad \text{on } \Gamma_1, \ldots, \Gamma_L \text{ and } \Gamma, \tag{2.25}$$

and with the open boundary conditions

$$\frac{\partial\Phi}{\partial z} = 0 \quad \text{on } \Gamma'. \tag{2.26}$$

The capability for the multiply connected domain is demonstrated through reconstructing the Southern Ocean circulation from the First Global Atmospheric Research Program (GARP) Global Experiment (FGGE) drifter buoy data, which is illustrated in Part II (Chu et al. 2003) of this paper.

3. Reconstruction procedure

a. Horizontal velocity

From the mathematical point of view, such a reconstruction can be reduced to a linear regression if normal and tangential velocities are given at the open boundary, and to a nonlinear regression otherwise. The regression coefficients are calculated from observed data.

The two scalar potentials are expanded into following Fourier series:

$$\Psi(x, y, z, t^\circ) = \sum_{k=1}^{\infty} a_k(z, t^\circ)\Psi_k(x, y, z, \kappa^\circ),$$

$$\frac{\partial\Phi(x, y, z, t^\circ)}{\partial z} = \sum_{m=1}^{\infty} b_m(z, t^\circ)\Phi_m(x, y, z), \tag{3.1}$$

where t° is the time of observations.

Substituting (3.1) into (2.4) and truncating modes at K and M for Ψ and Φ, respectively, we obtain an appropriate regression model through minimizing the following functional

$$J(a_1, \ldots, a_K, b_1, \ldots, b_M, \kappa, P) = \frac{1}{2}(\|u_p^{\text{obs}} - u_{KM}\|_P^2 + \|v_p^{\text{obs}} - v_{KM}\|_P^2) \to \min, \quad (3.2)$$

where u_p^{obs}, v_p^{obs} are observations at location p ($p = 1, \ldots, P$), P is the total number of observations, and

$$u_{KM} = \sum_{k=1}^{K} a_k(z, t^\circ)\frac{\partial \Psi_k(x, y, z, \kappa^\circ)}{\partial y} + \sum_{m=1}^{M} b_m(z, t^\circ)\frac{\partial \Phi_m(x, y, z)}{\partial x},$$

$$v_{KM} = -\sum_{k=1}^{K} a_k(z, t^\circ)\frac{\partial \Psi_k(x, y, z, \kappa^\circ)}{\partial x} + \sum_{m=1}^{M} b_m(z, t^\circ)\frac{\partial \Phi_m(x, y, z)}{\partial y}, \quad (3.3)$$

are reconstructed velocity components. Here, $\|\ldots\|_P$ is the P-dimensional Euclidean norm. After obtaining the spectral coefficients in (3.1) and parameterized κ, the horizontal velocity can be calculated for any point of the domain.

b. Vertical velocity and vorticity

For the reconstruction of vertical velocity at depth z^*, vertical differentiation is used on the second equation in (2.5):

$$\frac{\partial w}{\partial z} = -\Delta\frac{\partial \Phi}{\partial z}. \quad (3.4)$$

Equation (3.4) is integrated from the surface to the depth z^* or from the depth z^* to bottom and rewrite the result of integration as the following integral equation:

$$\iint G(x, x', y, y', z^*, t^\circ)w(x', y', z^*, t^\circ)\,dx'\,dy' - \iint G(x, x', y, y', z^*, t^\circ)w(x', y', 0, t^\circ)\,dx'\,dy' = \int_0^{z^*} \frac{\partial \Phi(x, y, z', t^\circ)}{\partial z'}\,dz', \quad (3.5)$$

where the Green function G and the vertical gradient of the poloidal potential $\partial\Phi/\partial z$ are given by

$$G(x, x', y, y', z, t^\circ) = \sum_{m=1}^{M} \mu_m^{-1}\Phi_m(x, y, z, t^\circ)\Phi_m(x', y', z, t^\circ), \quad (3.6)$$

$$\frac{\partial \Phi(x, y, z, t^\circ)}{\partial z} = \sum_{m=1}^{M} b_m(z, t^\circ)\Phi_m(x, y, z). \quad (3.7)$$

Equation (3.5) shows that to determine w, the vertical gradient of poloidal potential should be known on all horizons from surface to z^* or from z^* to bottom.

The same approach can be applied for the vertical vorticity:

$$\iint \tilde{G}(x, x', y, y', z, t^\circ)\xi(x', y', z, t^\circ)\,dx'\,dy' = \Psi(x, y, z, t^\circ), \quad (3.8)$$

where

$$\tilde{G}(x, x', y, y', z, t^\circ) = \sum_{k=1}^{K} \lambda_k^{-1}\Psi_k(x, y, z, t^\circ)\Psi_k(x', y', z, t^\circ), \quad \text{and} \quad (3.9)$$

$$\Psi(x, y, z, t^\circ) = \sum_{k=1}^{K} a_k(z, t^\circ)\Psi_k(x, y, z, t^\circ). \quad (3.10)$$

The series (3.6), (3.7), (3.9), and (3.10) converge rapidly.

c. Several steps in reconstruction

The reconstruction is generally divided into several steps: (a) parameterizing κ for the unknown open boundary condition, (b) reducing the optimization problem (3.2) to a linear regression model for a known open boundary condition or a nonlinear regression model for an unknown open boundary condition, (c) determining the optimal number of toroidal and poloidal modes in (3.3), and (d) estimating the reconstruction skill.

4. Regularization technique for solving the optimization problem

a. Spectral expansion of $\kappa(\tau)$

We expand $\kappa(\tau)$ along the open boundary Γ' into series:

$$\kappa(\tau) = \sum_{s=1}^{S} c_s T_s(\tau), \quad (4.1)$$

where T_s ($s = 1, \ldots, S$) are the continuous polynomials of $1, \tau, \tau^2, \ldots, \tau^S$ that are preliminarily orthogonalized along the open boundary.

For known (unknown) boundary conditions, a set of linear (nonlinear) regression equations is easily obtained from (3.2) to determine $K + M$ ($Q = K + M + S$) spectral coefficients from (3.3). The nonlinear regression is discussed here only since the nonlinear regression at each iteration uses the same technique as the linear regression. Thus, it is necessary to estimate $K + M$ spectral coefficients in (3.3) and S coefficients ($c_1, \ldots, c_S$) in (4.1).

b. Iteration process for nonlinear regression

The classical iteration approach (Eykhoff 1973) is used to the nonlinear regression equations. For the ith iteration,

$$\mathbf{h}^{[i+1]} = \mathbf{h}^{[i]} + \delta\mathbf{h}^{[i]}, \tag{4.2}$$

$$\mathbf{h}^{[i]} = (a_1^{[i]}, \ldots, a_K^{[i]}, b_1^{[i]}, \ldots, b_M^{[i]}, c_1^{[i]}, \ldots, c_S^{[i]})^{\mathrm{T}}, \tag{4.3}$$

where the increment $\delta\mathbf{h}^{[i]}$ is determined through minimizing the following functional:

$$J(\delta\mathbf{h}^{[i]}) = \frac{1}{2}\left\| u^{\mathrm{obs}} - u_{KM}(\mathbf{h}^{[i]}) - \frac{\partial u_{KM}}{\partial \mathbf{h}}\bigg|_{\mathbf{h}^{[i]}} \delta\mathbf{h}^{[i]} \right\|_P^2 + \frac{1}{2}\left\| v^{\mathrm{obs}} - v_{KM}(\mathbf{h}^{[i]}) - \frac{\partial v_{KM}}{\partial \mathbf{h}}\bigg|_{\mathbf{h}^{[i]}} \delta\mathbf{h}^{[i]} \right\|_P^2, \tag{4.4}$$

where the symbol $(,\ldots)^{\mathrm{T}}$ indicates the transpose operator. The iteration process (4.2)–(4.4) is divided into nine steps (Fig. 3). Detailed description is listed in appendix C.

At each iteration, determining $\delta\mathbf{h}^{[i]}$ is reduced to solving a set of ill-posed linear algebraic equations:

$$\mathbf{A}\delta\mathbf{h}^{[i]} = \mathbf{Y}, \tag{4.5}$$

where the coefficient matrix $\mathbf{A}$ is given by

$$A_{rq} = B_r B_q + C_r C_q; \qquad B_r = \frac{\partial u_{KM}}{\partial h_r}, \qquad C_r = \frac{\partial v_{KM}}{\partial h_r}, \qquad r, q = 1, \ldots, Q,$$

and the source vector $\mathbf{Y}$ is represented by

$$Y_r = [u^{\mathrm{obs}} - u_{KM}(\mathbf{h}^{[i]})]B_r + [v^{\mathrm{obs}} - v_{KM}(\mathbf{h}^{[i]})]C_r.$$

Here, MATLAB (1997) software is used to compute the basis functions $\{\Psi_k\}$ and $\{\Phi_m\}$ and adopt the same approach as Chu et al. (1997) to calculate B_r and C_r. Obviously, (4.5) is an ill-posed system and should be solved using a regularization method.

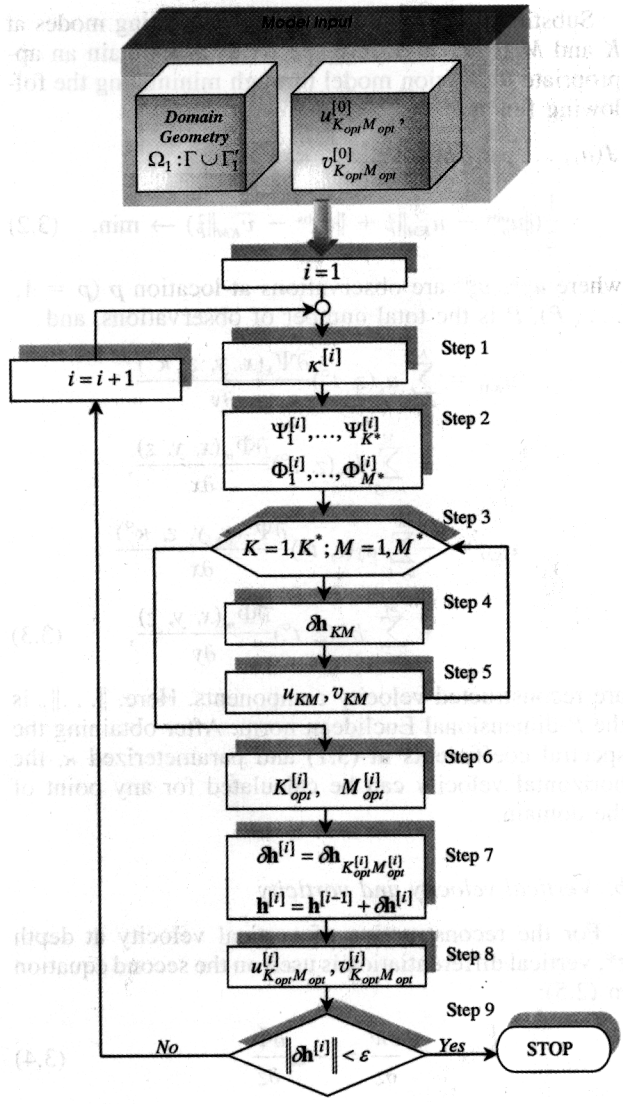

FIG. 3. Flowchart for determining the realization ($\mathbf{h}^{[i]}$) using the iteration process (4.2)–(4.4).

c. Stabilized least squares method

Numerous regularization techniques exist such as Golub's dumping high-order singular values, Tikhonov's regularization, iteration regularization, and others (see Engl et al. 1996). Most existing regularization techniques require a priori knowledge of statistical properties of noise and/or the structure of the solution of (4.5). Such a priori information is usually not available in oceanographic studies. Therefore, the methods that do not require this a priori knowledge are useful. The cross-validation method (e.g., Washba and Wendelberger 1980) is very popular in geophysical studies (e.g., Brankart and Brasseur 1996). However, it was found that the cross-validation approach often overdetermines the regularization parameter (Kugiumtzis et al. 1998; Ivanov et al. 2001a) and is highly sensitive to the size of observational samples used for the reconstruction (Mikhalsky 1987; Ivanov et al. 2001a). Thus, the stabilized least squares (SLS) method is used (Ivanov and Margolina 1996; Ivanov et al. 2001a).

This method constructs a special quasi-orthogonal rotation matrix $\mathbf{R}$ and multiplies it by the specially constructed linear system

$$\mathbf{R}\mathbf{A}'\delta\mathbf{h}^{[i]} = \mathbf{R}\mathbf{Y}', \tag{4.6}$$

such that $\mathbf{R}\mathbf{A}' \to \mathbf{A}_{\mathrm{reg}}$ and $\mathbf{R}\mathbf{Y}' \to \mathbf{Y}_{\mathrm{reg}}$, where $\mathbf{A}_{\mathrm{reg}}$ and $\mathbf{Y}_{\mathrm{reg}}$ are both regularized $Q \times Q$ matrix $\mathbf{A}$ and Q-dimensional observation vector $\mathbf{Y}$. Appendix B shows the procedure to construct the $Q \times 2P$ matrix $\mathbf{A}'$ and the $2P$-dimensional observation vector $\mathbf{Y}'$. A new transformed system (4.6) should have a much smaller noise-to-signal ratio η_1 and conditional number η_2 (the ratio of the maximum to minimum singular values of the system matrix).

The rotation matrix is constructed as the limit of plane rotation matrices (Givens matrices):

$$\mathbf{R} = \lim_{J\to\infty} \prod_{j=1}^{J} \left(R_{2P,2P-1}^{[j]} \cdots \prod_{p=3}^{2P} R_{2p}^{[j]} \prod_{p=2}^{2P} R_{1p}^{[j]} \right), \quad (4.7)$$

where $R_{qp}^{[j]}$ is Givens matrix at jth iteration applied to qth and pth lines. The rotation angles ($\varphi_{qp}^{[j]}$) of $R_{qp}^{[j]}$ are determined through the following maximization process:

$$J_r(\varphi_{qp}^{[j]}) = \sum_{q=1}^{Q} (R_{rp}^{[j]} a_{qp}^{[j-1]})^2 \|\delta\mathbf{h}_{\text{eff}}\|_Q^2 - (R_{rp}^{[j]} Y_p^{[j-1]})^2 \to \max,$$

$$a_{qp}^{[0]} = a_{qp}, \qquad Y_p^{[0]} = Y_p, \quad (4.8)$$

with $\|\delta\mathbf{h}_{\text{eff}}\|_Q^2$ called the effective norm.

This norm is determined by

$$\tilde{J} = \left(\frac{\|\delta\hat{\mathbf{h}}^{[l]}\|^2}{\|\delta\mathbf{h}_{\text{eff}}\|^2} - 1 \right)^2 \to \min, \quad (4.9)$$

where $\delta\hat{\mathbf{h}}^{[l]}$ is a regularized solution of the transformed system (4.6). Iteration is used to solve (4.8) and (4.9) with an empirical requirement:

$$1.5P < Q < 2P.$$

See Ivanov et al. (2001a) for detailed information.

d. Properties of the rotation matrix

To construct the linear transformation $\mathbf{R}$, we do not need a priori knowledge on statistical properties of noise. However, the best results are obtained if the exact observational (no error) vector $\mathbf{Y}_{\text{exact}}$ is perpendicular to the noise vector $\mathbf{Y}_{\text{noise}}$; that is, the inner product is equal to 0:

$$\mathbf{Y}_{\text{exact}} \cdot \mathbf{Y}_{\text{noise}} = 0,$$

which indicates no interference between noise and the exact observational vectors.

For a high conditional number, the rotation matrix algorithm (4.6)–(4.9) has the same accuracy as Tikhonov et al.'s (1995) technique for selecting the optimal regularization parameter (Ivanov et al. 2001a). For a small condition number ($\eta_2 \to 1$), the estimate using the SLS method has the same accuracy as the classical least squares (LES) solution (4.4) when the noise-to-signal ratio is small ($\eta_1 \to 0$), and has much better accuracy than the LES estimation when the noise-to-signal ratio is large ($\eta_1 \gg 0$).

The accuracy of the approach is estimated by

$$\text{cov}(\delta\hat{\mathbf{h}}) = (\mathbf{R}^T\mathbf{A}')^{-1}\mathbf{R}^T\boldsymbol{\Omega}\mathbf{R}(\mathbf{R}^T\mathbf{A}')^{-1}, \quad (4.10)$$

where $\boldsymbol{\Omega}$ is the noise covariance matrix, which is usually unknown, and which makes (4.10) less practical.

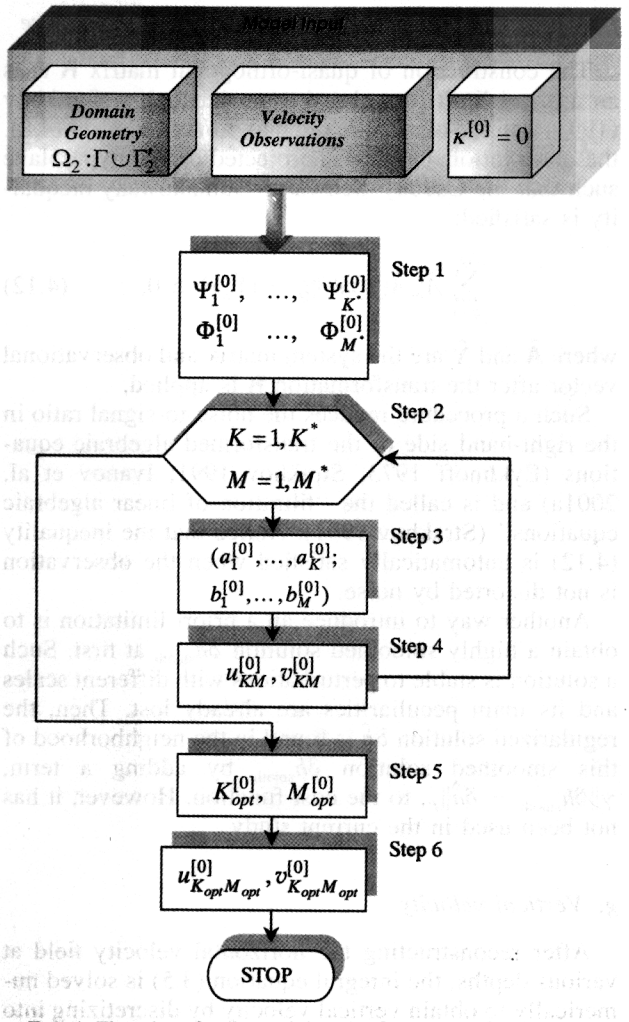

FIG. 4. Flowchart for determining the first guess ($\delta\mathbf{h}^{[0]}$) for the iteration process (4.2)–(4.4).

e. First guess for the iteration process

It is well known that the iteration process (4.2)–(4.4) (shown in Fig. 3) may be divergent if the first guess $\delta\mathbf{h}^{[0]}$ is far from reality. Therefore, to have a good estimate of $\delta\mathbf{h}^{[0]}$ becomes important. A boundary extension method is proposed to determine the initial guess values of the spectral coefficients. Let the domain (Ω_1) have an open boundary Γ_1'. The domain Ω_1 is extended into Ω_2 ($\Omega_1 \subset \Omega_2$) with an open boundary Γ_2' (Fig. 1) such that

$$\left.\frac{\partial\Psi}{\partial n}\right|_{\Gamma_2'} = 0, \qquad \left.\frac{\partial\Phi}{\partial z}\right|_{\Gamma_2'} = 0. \quad (4.11)$$

The circulation is reconstructed in Ω_2 using (4.5) from appropriate linear regression model at first. Then, with the known velocity field at Γ_1', we determine κ using (2.9) and obtain $\delta\mathbf{h}^{[0]}$ for the domain Ω_1. Figure 4 shows the flowchart for determining $\delta\mathbf{h}^{[0]}$. Detailed description of the process is listed in appendix D.

f. A priori limitation in the regularization procedure

The construction of quasi-orthogonal matrix **R** uses an a priori limit formulated as an inequality. Strakhov (1991) pointed out that in the maximizing process (4.8), the observational vector is projected onto a hyperplane such that the Cauchy–Schwartz–Buniakowsky inequality is satisfied:

$$\sum_{q=1}^{Q} \tilde{A}'_{pr}\tilde{A}'_{rq}\|\delta h^{(i)}\|_Q^2 - (\tilde{Y}'_p)^2 \geq 0, \qquad (4.12)$$

where $\tilde{\mathbf{A}}$ and $\tilde{\mathbf{Y}}$ are the system matrix and observational vector after the transformation **R** is applied.

Such a procedure reduces the noise-to-signal ratio in the right-hand side of the transformed algebraic equations (Eykhnoff 1973; Strakhov 1991; Ivanov et al. 2001a) and is called the "filtration of linear algebraic equations" (Strakhov 1991). Notice that the inequality (4.12) is automatically satisfied when the observation is not distorted by noise.

Another way to introduce an a priori limitation is to obtain a highly smoothed solution δh_{smoth} at first. Such a solution is stable to perturbations with different scales and its main peculiarities are already lost. Then, the regularized solution $\delta\hat{h}$ is found in the neighborhood of this smoothed solution δh_{smoth} by adding a term, $\gamma\|\delta h_{\text{smoth}} - \delta\hat{h}\|_P$, to the cost function. However, it has not been used in the current study.

g. Vertical velocity

After reconstructing the horizontal velocity field at various depths, the integral equation (3.5) is solved numerically to obtain vertical velocity by discretizing into a set of algebraic equations in the ordinary way (Tikhonov et al. 1995):

$$\mathbf{Gw} = \mathbf{z}, \qquad (4.13)$$

where **G** is a coefficient matrix, and **w** and **z** are vectors. Their dimensions are determined by the discretization of (3.5). Since **G** is usually a square matrix, the SLS method cannot be used to regularize the ill-posed system (4.13).

Tikhonov et al. (1995) change (4.13) into an optimization process:

$$\|\mathbf{Gw} - \mathbf{z}\|^2 + \delta\|\mathbf{w}\|^2 \to \min, \qquad (4.14)$$

where δ is the regularization parameter. Here, the minimum sensitivity of the solution to δ is used to determine its value without the knowledge of the low-order noise statistics. Baglai (1986) pointed out that this method is equivalent to classical Tikhonov's method in determining δ.

h. Summation of the Fourier series

Usually, the calculated Fourier coefficients $\{a_k(z, t)\}$, $\{b_m(z, t)\}$ contain errors. If the errors are large, the summation of the Fourier series in (3.6), (3.7), (3.9), and (3.10) needs to be regularized [taking (3.7) as an example]. Such a regularization is achieved through multiplying each term of the series by a weight factor (Strahkov and Valyashko 1981):

$$\frac{\partial\Phi}{\partial z} = \sum_{m=0}^{M} \frac{\mu_m^2(z)}{\mu_m^2(z) + \delta\Lambda_m^2(z)} b_m(z, t)\Phi_m(x, y, z), \qquad (4.15)$$

where Λ_m is chosen as

$$\Lambda_m^{-1} = \frac{|b_m|}{\max(|b_m|)}.$$

Such a process strongly smooths out the low-energy modes and keeps the high-energy modes in (4.15). Herein, also, δ is estimated from sensitivity ideas.

5. Estimation of reconstruction skill and choice of model parameters (*K, M, S*)

a. Vapnik–Chervonkis cost function

Theoretically, the reconstruction skill should be estimated through the statistical cost function $\langle J\rangle$, determined as

$$\langle J\rangle = \frac{1}{2}\left[\iint (u - u_{KM})^2 f_1(u, v|x, y) f_2(x, y)\, du\, dv\, dx\, dy + \iint (v - v_{KM})^2 f_1(u, v|x, y) f_2(x, y)\, du\, dv\, dx\, dy\right], \qquad (5.1)$$

where $f_1(u, v \mid x, y)$ and $f_2(x, y)$ are both the probability density functions for the velocity and station disposition inside the domain, respectively; the angle brackets ($\langle\,\rangle$) denote the ensemble average over realizations of u and v.

For a limited number of data (P finite), the ensemble average is replaced by the empirical average over all observational points. This leads to the empirical cost function

$$J_{\text{emp}} = J(a_1, \ldots, a_K, b_1, \ldots, b_M, \kappa, P). \qquad (5.2)$$

For a large number of data ($P \to \infty$), the coefficients $\{\hat{a}_1, \ldots, \hat{a}_K, \hat{b}_1, \ldots, \hat{b}_M, \hat{\kappa}\}$ obtained by minimizing J_{emp} coincide with the coefficients $\{a_1^*, \ldots, a_K^*, b_1^*, \ldots, b_M^*, \kappa^*\}$ obtained by minimizing $\langle J \rangle$. However, this is not true for the limited data.

Vapnik (1983) suggested to estimate the difference between J_{emp} and $\langle J \rangle$ by the probabilistic approach. He found that the probability of the maximum difference between the empirical and ensemble cost functions being larger than a given tolerance μ should be less than some level g, which tends to zero as the observational sample size tends to infinity:

$$\text{Prob}\left\{\sup_{K,M,S} |\langle J(K, M, S)\rangle - J_{emp}(K, M, S)| \geq \mu\right\} \leq g(P, \mu) \tag{5.3}$$

$$\lim_{P\to\infty} g(P, \mu) = 0, \tag{5.4}$$

where "Prob" denotes the probability. From (5.3) we have

$$J_{emp}(K, M, S) - \mu \leq \langle J(K, M, S)\rangle \leq J_{emp}(K, M, S) + \mu, \tag{5.5}$$

which leads to a formula for so-called Vapnik–Chervonkis cost function (VCCF):

$$J_{KMS} = J_{emp}(K, M, S) + \mu. \tag{5.6}$$

The tolerance μ depends on the chosen numerical model and is determined by two criteria: (a) minimization of the probability (5.3), and (b) uniform convergence of the coefficient set

$$\{\hat{a}_1, \ldots, \hat{a}_K, \hat{b}_1, \ldots, \hat{b}_M, \hat{\kappa}\} \text{ to } \{a_1^*, \ldots, a_K^*, b_1^*, \ldots, b_M^*, \kappa^*\} \quad \text{as } P \to \infty.$$

b. Optimal spectral truncation

Vapnik's (1983) method is used to determine the optimal values for three model parameters ($K_{opt}, M_{opt}, S_{opt}$). For simplicity without loss of generality, we illustrate the approach with a given S_{opt}. Let the family of models

$$(u_{K0}, v_{K0}), (u_{K1}, v_{K1}), (u_{K2}, v_{K2}), \ldots, (u_{KM}, v_{KM})$$

be used in the reconstruction process. The velocity component (u_{K0}, v_{K0}) does not contain contribution from the poloidal potential (i.e., $b_0 = 0$). The optimal parameter K_{opt} is determined through minimization of the functional

$$J_{Km} = J_{emp} + 2\hat{J}_m\left\{\frac{K}{P}\left[\ln\left(\frac{2P}{K}\right) + 1\right] - \frac{\ln(g)}{P}\right\}^{1/2}, \quad m = 0, \ldots, M, \tag{5.7}$$

where $g = 0.95$ and

$$\sup_{a_1,\ldots,a_K,b_1,\ldots,b_M,\kappa,x,y} \frac{1}{2}[(u^{obs} - u_{Km})^2 + (v^{obs} - v_{Km})^2] \leq \hat{J}_m. \tag{5.8}$$

Then, the optimal parameter M_{opt} should be obtained through the minimization process:

$$J_{K_{opt}M_{opt}} = \min(J_{K_{opt}0}, J_{K_{opt}1}, J_{K_{opt}2}, \ldots, J_{K_{opt}M}). \tag{5.9}$$

The reconstructed field $\{u(K_{opt}, M_{opt}), v(K_{opt}, M_{opt})\}$ is the solution that guarantees the minimum difference between $\langle J \rangle$ and J_{emp} for a given observational sample size. It is noticed that the less the difference between $\langle J \rangle$ and J_{emp}, the closer the truncated mode $\{u_{KM}, v_{KM}\}$ is to reality.

From the physical point of view, the optimal parameters are found through the cost function (5.9), which is a trade-off between the likelihood of a model (i.e., its ability to reproduce data) and a penalty for making the model too complex for the data.

c. Root-mean-square error

When the exact solution is known, we used the root-mean-square error (rmse) inside the domain:

$$\chi_u = \left\{\iint \frac{(u_{ex} - u_{KM})^2}{\langle u_{ex}^2\rangle}\, dx\, dy\right\}^{1/2}, \quad \chi_v = \left\{\iint \frac{(v_{ex} - v_{KM})^2}{\langle v_{ex}^2\rangle}\, dx\, dy\right\}^{1/2}, \tag{5.10}$$

and along the open boundary:

$$\chi_n = \left\{\oint_{\Gamma_i'} \frac{(V_n - \hat{V}_n)^2}{\langle V_n^2\rangle}\, d\tau'\right\}^{1/2}, \quad \chi_\tau = \left\{\oint_{\Gamma_i'} \frac{(V_\tau - \hat{V}_\tau)^2}{\langle V_\tau^2\rangle}\, d\tau'\right\}^{1/2}, \tag{5.11}$$

to determine the reconstruction skill. Here, u_{ex}, v_{ex}, V_n, and V_τ represent the exact velocity components, $(\hat{})$ denotes the reconstructed field, and $\langle \ldots \rangle$ is the averaging operator over the domain or along the open boundary. To estimate spatial structure of reconstruction error, the residual velocity defined by Lipphardt et al. (2000),

$$\mathbf{u}_{res} = \mathbf{u}_{ex} - \mathbf{u}_{KM}, \tag{5.12}$$

is used. It is noticed that such a skill is on the base of the known exact velocity $\mathbf{u}_{ex}$ and (V_n, V_τ) and has little practical significance. However, it is applicable for verification in identical twin experiments.

6. Computational cost

Flow reconstruction is performed by solving a set of $(K + M)I$ linear algebraic equations (3.3) for the zero-order approximation case and by solving a set of $(K +$

$M + S)(K + M + S)II_1 + (K + M + S)II_1$ linear algebraic equations (4.1)–(4.5) for iteration process for nonlinear regression. Here, I and I_1 are the numbers of iteration to determining $\mathbf{h}^{[i]}$ and (K_{opt}, M_{opt}), respectively. Thus, computational cost depends on the selection of the optimal modes (the basis functions) used in the spectral decomposition. In general, the number of the basis functions determines the smoothness of the reconstructed circulation (Courant and Hilbert 1966).

In additional to the three examples presented in Part II of this paper, the spectral decomposition (2.11)–(2.17) was performed for the Black Sea with horizontal resolution of 18 km (Eremeev et al. 1992a,b); for the Gulf of Mexico with horizontal resolution of 9 km (Chu et al. 2003); for the Monterey Bay with horizontal resolution of 1 km (Ivanov and Melnichenko 2002); and for Louisiana–Texas shelf with horizontal resolution of 10 km (Ivanov et al. 2001b). In these calculations, the optimal number of basis functions are

$$K_{opt} = 40, \quad M_{opt} = 30, \quad S = 0,$$

for the Black Sea reconstruction [closed basin, with the boundary conditions (2.11), (2.12)];

$$K_{opt} = 120, \quad M_{opt} = 20, \quad S_{opt} = 5,$$

for the Gulf of Mexico reconstruction [semiclosed basin, with the open boundary conditions (2.10), (2.13)];

$$K_{opt} < 70, \quad M_{opt} < 20,$$

for the Monterey Bay reconstruction [with the open boundary conditions (2.10), (2.13), and (2.18)]; and

$$K_{opt} < 40, \quad M_{opt} < 10, \quad S_{opt} = 3,$$

for the Louisiana–Texas shelf reconstruction [open shelf area, with the simplified open boundary conditions (2.18)]. If the zero-order approximation (first guess) is successfully chosen, the numbers of iteration, I and I_1, usually do not exceed 7. If they are larger than 7, the simplified open boundary conditions (2.18) is recommended.

In reconstructing the Gulf of Mexico circulation on a Pentium-III (850 MHz) processor, 300 toroidal and poloidal basis functions are determined (40 CPU min) from a 15 400 × 15 400 matrix corresponding to 2D Laplacian with the Gulf of Mexico geometry. A set of 10^5 linear algebraic equations is solved at each iteration in (4.2)–(4.5) using a special technique for super large linear algebraic system developed by Strakhov and Strakhov (1999). Such calculation consumes about 5.6 CPU h. The relatively high computational cost is caused by the use of large data with the total open boundary conditions (2.10) and (2.13). If the simple open boundary condition (2.10) is used, the computational cost is greatly reduced.

7. Conclusions

First, a multistep scheme is developed to reconstruct velocity from sparse and noisy data in an open domain: (a) a boundary extension method to determine normal and tangential velocities at an open boundary, (b) establishment of homogeneous open boundary conditions for the two potentials with a spatially varying coefficient $\kappa(\tau)$, (c) spectral expansion of $\kappa(\tau)$, (d) determination of basis functions for the two potentials for the spectral decomposition using homogeneous boundary conditions, and (e) determination of coefficients in the spectral decomposition of velocity and $\kappa(\tau)$ using linear or nonlinear regressions.

Second, the homogeneous boundary conditions of (Ψ, Φ) at both rigid and open boundary segments make it possible to obtain basis functions for an open domain. The basis functions are the eigenfunctions of the Laplacian operator with homogeneous boundary conditions and depend on the spectrally varying parameter κ at the open boundary.

Third, the spectra of the two horizontal velocity components and κ are truncated at K, M, and S. The optimal model parameters (K_{opt}, M_{opt}, S_{opt}) are determined through a modified cost function, which is constructed on the basis of model capability and data reproduction complexity (penalty). This cost function is also used to verify the model reconstruction skill from sparse and noisy data.

Fourth, the spectral coefficients for horizontal velocity and κ are determined simultaneously using the stabilized least squares (SLS) method. This method does not require a priori knowledge about noise and is robust to the size of observational samples used for the reconstruction.

Fifth, after reconstructing the horizontal velocity field at various depths, the vertical velocity may be reconstructed through solving the integral equation (3.5) numerically. Since the coefficient matrix is square, the minimum sensitivity of solution is used to determine the regularization parameter and then use Tikhonov's approach to reconstruct the vertical velocity.

Acknowledgments. The authors are grateful to Professor Christopher N. K. Mooers at the University of Miami for invaluable suggestions. Ivanov thanks Professor A. D. Kirwan Jr. for fruitful discussions about the problem of open boundary conditions. The authors are also grateful to anonymous reviewers for helpful comments.

This research was sponsored by the Office of Naval Research, Naval Oceanographic Office, and the Naval Postgraduate School. Leonid Ivanov, Tatyana Korzhova, Tatyana Margolina, and Oleg Melnichenko thank U.S. Civilian Research and Development Foundation for support received through Award UG-2079. Leonid Ivanov also thanks the International Field Office of the Office of Naval Research for support under the Grant N00014-02-1-4058. This work was partially conducted by Leonid Ivanov while he held a National Research Council Research Associateship Award at the Naval Postgrad-

uate School, and while he visited the University of Delaware.

APPENDIX A

Two-Scalar Potential Representation of Three-Dimensional Incompressible Flow

Consider spherical coordinates with $\mathbf{r}$ representing the radius vector. Using the Helmholtz theorem (Morse and Feshbach 1953), the horizontal velocity at a given radius $|\mathbf{r}| = r$ is written as

$$\mathbf{u}_H = \mathbf{r} \times \nabla_H A_1 + \nabla_H A_3, \tag{A.1}$$

where ∇_H is the two-dimensional nabla operator.

Let us define a new function A_2 such that the radial velocity component is written by

$$u_r = rA_2 + \frac{\partial A_3}{\partial r}. \tag{A.2}$$

Combination of (A.1) and (A.2) gives a well-known form for a three-dimensional vector field (Dubrovin et al. 1992):

$$\mathbf{u} = \mathbf{r} \times \nabla A_1 + \mathbf{r}A_2 + \nabla A_3. \tag{A.3}$$

To reduce the number of scalar functions in (A.3) from 3 to 2, two fundamental properties of oceanic flows are accounted for 1) existence of the vertical axis marked out by the earth's rotation for large-, meso- and submesoscales; and 2) incompressibility.

The first property of ocean flows allows to construct the unique invariant transformation for (A.1) and (A.2):

$$\tilde{A}_1 = A_1 - f_1(r), \qquad \tilde{A}_2 = A_2 + \frac{1}{r}\frac{df_2(r)}{dr},$$
$$\tilde{A}_3 = A_3 - f_2(r), \tag{A.4}$$

where f_1 and f_2 are two arbitrary functions depending on r only. In general, the three-dimensional flow is decomposed by

$$\mathbf{u} = \mathbf{r} \times \nabla\tilde{A}_1 + \mathbf{r}\tilde{A}_2 + \nabla\tilde{A}_3. \tag{A.5}$$

Two velocity components,

$$\mathbf{u}^{\text{tor}} = \mathbf{r} \times \nabla\tilde{A}_1 = \nabla \times (\mathbf{r}\tilde{A}_1), \quad \text{and}$$
$$\mathbf{u}^{\text{pol}} = \mathbf{r}\tilde{A}_2 + \nabla\tilde{A}_3, \tag{A.6}$$

are also invariant in the transform (A.3). The two components $\mathbf{u}^{\text{tor}}$ and $\mathbf{u}^{\text{pol}}$ are called the toroidal and poloidal velocities (Moffat 1978), respectively. Substitution of (A.3) into the incompressibility condition

$$\nabla \cdot \mathbf{u} = 0$$

leads to the following relationship:

$$\Delta\tilde{A}_3 = -\nabla(\mathbf{r}\tilde{A}_2). \tag{A.7}$$

According to (A.6), the poloidal potential Φ of the field can be defined by

$$\mathbf{r}\tilde{A}_2 + \nabla\tilde{A}_3 = \nabla \times \nabla \times (\mathbf{r}\Phi). \tag{A.8}$$

Let $\tilde{A}_1 = \Psi$, then (A.3) becomes

$$\mathbf{u} = \nabla \times (\mathbf{r}\Psi) + \nabla \times \nabla \times (\mathbf{r}\Phi), \tag{A.9}$$

which is the two-scalar representation for a three-dimensional incompressible field. For more details, see Moffat (1978) and Zeldovich et al. (1985). Obviously, the two potentials (Ψ, Φ) defined here are not the same as the streamfunction (A_1) and velocity potential (A_3) of a two-dimensional flow $\mathbf{u}_H$ on a spherical surface.

APPENDIX B

Structure of A' and Y' in (4.5)

The matrix $\mathbf{A}'$ and the vector $\mathbf{Y}'$ in (4.6) are given by

$$\mathbf{A}' = \begin{pmatrix} \left.\frac{\partial u_{NM}}{\partial h_1}\right|_{p=1} & \cdots & \left.\frac{\partial u_{NM}}{\partial h_Q}\right|_{p=1} \\ \cdots & \cdots & \cdots \\ \left.\frac{\partial u_{NM}}{\partial h_1}\right|_{p=P} & \cdots & \left.\frac{\partial u_{NM}}{\partial h_Q}\right|_{p=P} \\ \left.\frac{\partial v_{NM}}{\delta h_1}\right|_{p=1} & \cdots & \left.\frac{\partial v_{NM}}{\partial h_Q}\right|_{p=1} \\ \cdots & \cdots & \cdots \\ \left.\frac{\partial v_{NM}}{\partial h_1}\right|_{p=P} & \cdots & \left.\frac{\partial v_{NM}}{\partial h_Q}\right|_{p=P} \end{pmatrix};$$

$$\mathbf{Y}' = \begin{pmatrix} u^{\text{obs}} - u_{KM}(\mathbf{h}^{[i]})|_{p=1} \\ \cdots \\ u^{\text{obs}} - u_{KM}(\mathbf{h}^{[i]})|_{p=P} \\ v^{\text{obs}} - v_{KM}(\mathbf{h}^{[i]})|_{p=1} \\ \cdots \\ v^{\text{obs}} - v_{KM}(\mathbf{h}^{[i]})|_{p=P} \end{pmatrix}. \tag{B.1}$$

After multiplying R to the system (4.5) we have

$$\mathbf{A}_{\text{reg}} = \begin{pmatrix} a_{11} & \cdots & a_{1Q} & \ominus \\ \cdots & \cdots & \cdots & \ominus \\ a_{Q1} & \cdots & a_{QQ} & \ominus \\ \ominus & \ominus & \ominus & \ominus \\ c_{2P1} & \cdots & \cdots & c_{2P2P} \end{pmatrix}; \qquad \mathbf{Y}_{\text{reg}} = \begin{pmatrix} b_1 \\ \cdots \\ b_Q \\ 0 \\ d_{2P2P} \end{pmatrix}. \tag{B.2}$$

Here, the last rows in $\mathbf{A}_{\text{reg}}$ and $\mathbf{Y}_{\text{reg}}$ are excluded from the analysis because they are not filtered. The transformed system (4.6) is well posed and can be solved using a typical linear algebraic method such as the Gauss procedure.

APPENDIX C

Determination of the Realization ($\mathbf{H}^{[i]}$)

This process starts from the first-guess optimal velocity ($u^{[0]}_{K_{opt}M_{opt}}$, $v^{[0]}_{K_{opt}M_{opt}}$) in the domain Ω_1 ($\Gamma \cup \Gamma_1'$). There are nine steps (for iteration i) to determine the realization ($\mathbf{h}^{[i]}$) (Fig. 3).

1) Calculate $\kappa^{[i]}$ ($i = 1, 2, \ldots$) along the open boundary Γ_1' for the domain Ω_1 ($\Gamma \cup \Gamma_1'$).
2) Determine the basis functions $\{\Psi_1^{[i]}, \Psi_2^{[i]}, \ldots, \Psi_K^{[i]}\}$ and $\{\Phi_1^{[i]}, \Phi_2^{[i]}, \ldots, \Phi_M^{[i]}\}$ for the domain Ω_1 with $\kappa^{[i]}$.
3) Calculate the velocity ($u^{[i]}_{KM}$, $v^{[i]}_{KM}$) for the pair of (K, M). Determine the optimal pair (K_{opt}, M_{opt}) through minimizing the Vapnik–Chervonkis cost function (5.6). Then, obtain the optimal adjustment $\delta\mathbf{h}^{[i]}_{K_{opt}M_{opt}}$ using (4.6).
4) Update the vector $\mathbf{h}^{[i]}$.
5) Compute the optimal velocity ($u^{[i]}_{K_{opt}M_{opt}}$, $v^{[i]}_{K_{opt}M_{opt}}$).
6) Compare $\|\delta\mathbf{h}^{[i]}\|$ with the tolerance level ε. If $\|\delta\mathbf{h}^{[i]}\| < \varepsilon$, the iteration stops, and ($u^{[i]}_{K_{opt}M_{opt}}$, $v^{[i]}_{K_{opt}M_{opt}}$) is the final reconstructed velocity field. If $\|\delta\mathbf{h}^{[i]}\| \geq \varepsilon$, the next step iteration starts.

APPENDIX D

Determination of the First Guess ($\delta\mathbf{H}^{[0]}$)

This process starts from noisy observational velocity data in the expanded domain Ω_2 ($\Gamma \cup \Gamma_2'$) with the assumption $\kappa^{[0]} = 0$. There are five steps to determine the first guess ($\delta\mathbf{h}^{[0]}$) (Fig. 4).

1) Calculate the two sets of the basis functions $\{\Psi_1^{[0]}, \Psi_2^{[0]}, \ldots, \Psi_K^{[0]}\}$ and $\{\Phi_1^{[0]}, \Phi_2^{[0]}, \ldots, \Phi_M^{[0]}\}$ using the Lanchoz–Arnoldi method from MATLAB 6.0.
2) Calculate the velocity ($u^{[0]}_{KM}$, $v^{[0]}_{KM}$) for the pair of (K, M) using (3.3). Determine the optimal pair (K_{opt}, M_{opt}) through minimizing the Vapnik–Chervonkis cost function (5.6). Detailed explanation of this procedure can be found in section 5b.
3) Compute the first-guess optimal velocity ($u^{[0]}_{K_{opt}M_{opt}}$, $v^{[0]}_{K_{opt}M_{opt}}$) using (3.3).

REFERENCES

Baglai, P. D., 1986: Using sensitivity functions for the choice of regularization parameter. *Sov. J. Comput. Math. Phys.*, **15,** 305–320.

Brankart, J.-M., and P. Brasseur, 1996: Optimal analysis of in situ data in the western Mediterranean using statistics and cross-validation. *J. Atmos. Oceanic Technol.*, **13,** 476–491.

Cho, K., R. O. Reid, and W. D. Nowlin Jr., 1998: Objectively mapped stream function fields on the Texas–Louisiana shelf based on 32 months of moored current meter data. *J. Geophys. Res.*, **103,** 10 337–10 390.

Chu, P. C., 1999: Fundamental circulation functions for determination of open boundary conditions. Preprints, *Third Conf. on Coastal Atmospheric and Oceanic Prediction and Processes,* New Orleans, LA, Amer. Meteor. Soc., 389–394.

——, C. Fan, and L. L. Ehret, 1997: Determination of open boundary conditions with an optimization method. *J. Atmos. Oceanic Technol.*, **14,** 1066–1071.

——, L. M. Ivanov, L. H. Kantha, O. V. Melnichenko, and Y. A. Poberezhny, 2002: Power law decay in model predictability skill. *Geophys. Res. Lett.*, **29** (15), 1748, doi:10.1029/2002GL014891.

——, L. M. Ivanov, T. P. Korzhova, T. M. Margolina, and O. V. Melnichenko, 2003: Analysis of sparse and noisy ocean current data using flow decomposition. Part II: Applications to Eulerian and Lagrangian data. *J. Atmos. Oceanic. Technol.*, **20,** 492–512.

Courant, R., and D. Hilbert, 1966: *Methods of Mathematical Physics.* Vol. II. Wiley-Interscience, 502 pp.

Davis, R. E., 1985: Objective mapping by least square fitting. *J. Geophys. Res.*, **90,** 4773–4777.

Dubrovin, B. A., A. T. Fomenko, and S. P. Novikov, 1992: *Modern Geometry—Methods and Applications.* Springer-Verlag, 469 pp.

Engl, H. W., M. Hanke, and A. Neubauer, 1996: *Regularization of Inverse Problems—Mathematics and Its Applications.* Kluwer, 321 pp.

Eremeev, V. N., L. M. Ivanov, and A. D. Kirwan Jr., 1992a: Reconstruction of oceanic flow characteristics from quasi-Lagrangian data. Part 1. Approach and mathematical methods. *J. Geophys. Res.*, **97,** 9733–9742.

——, ——, S. V. Kochergin, and O. V. Melnichenko, 1992b: Seasonal variability and the types of currents in the upper layer of the Black Sea. *Sov. J. Phys. Oceanogr.*, **3,** 193–208.

Eykhoff, P., 1973: *System Identification: Parameter and State Estimation.* Elsevier, 555 pp.

Flierl, G. R., 1977: Simple applications of McWilliams' "A note on a consistent quasigeostrophic model in a multiply connected domain." *Dyn. Atmos. Oceans,* **1,** 443–453.

Gandin, L. S., 1965: *Objective Analysis of Meteorological Fields.* Israel Program for Scientific Translation, 242 pp.

Inoue, H., 1986: A least-squares, smooth fitting for irregularly spaced data: Finite-element approach using the cubic B-spline basis. *Geophysics,* **51,** 2051–2066.

Ivanov, L. M., and T. M. Margolina, 1996: Reconstruction of oceanographic fields without an information on statistical properties of noise. Preprints, *First Conf. on Coastal Oceanic and Atmospheric Prediction,* Atlanta, GA, Amer. Meteor. Soc., 155–158.

——, and O. V. Melnichenko, 2002: Nowcast of surface currents from blending HF radar: Inverse model, application to Monterey Bay. *Proc. IGARSS'02.*

——, A. D. Kirwan Jr., and T. M. Margolina, 2001a: Filtering noise from oceanographic data with some applications for the Kara and Black Seas. *J. Mar. Syst.*, **28,** 113–139.

——, T. M. Margolina, and O. V. Melnichenko, 2001b: Reconstruction of large-, meso- and submeso-scale structures in ocean from the moored current meter and drifter data. *Proc. Int. Conf. on Fluxes and Structure in Fluids,* 134–140.

Kamenkovich, V. M., 1961: The integration of the marine current theory equations in multiply connected regions (in Russian). *Dokl. Akad. Nauk USSR,* **138,** 629–631.

Kugiumtzis, D., O. C. Lingjarde, and N. Christophersen, 1998: Regularized local linear prediction of chaotic time series. *Physica D,* **112,** 344–360.

Ladyzhenskaya, O. A., 1969: *Mathematical Problems of Viscous Incompressible Flows.* Gordon and Breach, 224 pp.

Lipphardt, B. L., Jr., A. D. Kirwan Jr., C. E. Grosch, L. M. Ivanov, and J. K. Lewis, 1997: Merging disparate ocean data. *Rapid Environmental Assessment,* E. Pouliquen, A. D. Kirwan, and R. T. Pearson, Eds., NATO SACLANT Undersea Research Center, 211–218.

——, ——, ——, J. K. Lewis, and J. D. Paduan, 2000: Blending HF radar and model velocities in Monterey Bay through normal mode analysis. *J. Geophys. Res.*, **105,** 3425–3450.

Lynch, P., 1988: Deducing the wind from vorticity and divergence. *Mon. Wea. Rev.*, **116,** 86–93.

Malanotte-Rizzoli, P., and E. Tziperman, 1996: The oceanographic data assimilation problem: Overview, motivation and purposes. *Modern Approaches to Data Assimilation in Ocean Modeling,* P. Malonotte-Rizzoli, Ed., Elsevier, 3–17.

MATLAB, 1997: *High-Performance Numeric Computation and Visualization Software,* The Math Works, Inc., 548 pp.

McWilliams, J. C., 1977: A note on a consistent quasigeostrophic model in a multiply connected domain. *Dyn. Atmos. Oceans,* **1,** 427–441.

Mikhalsky, A. I., 1987: Choice of an evaluation algorithm using samples of limited size (in Russian). *Avtom. Telemekh.,* **7,** 91–102.

Moffat, H. K., 1978: *Magnetic Field Generation in Electrically Conducting Fluids.* Cambridge University Press, 578 pp.

Morse, P. M., and H. Feshbach, 1953: *Methods of Theoretical Physics.* McGraw-Hill, 997 pp.

Pedersen, K., 1971: Balanced systems of equations for the atmospheric motion. *Geofys. Publ.,* **28,** 1–12.

Rao, D. B., and D. J. Schwab, 1981: A method of objective analysis for currents in a lake with application to Lake Ontario. *J. Phys. Oceanogr.,* **11,** 739–750.

Seiler, U., 1993: Estimation of open boundary conditions with the adjoint method. *J. Geophys. Res.,* **98,** 22 855–22 870.

Shulman, I., and J. K. Lewis, 1995: Optimization approach to the treatment of open boundary conditions. *J. Phys. Oceanogr.,* **25,** 1006–1011.

Smith, W. H., and P. Wessel, 1990: Gridding with continuous curvature splines in tension. *Geophysics,* **55,** 293–305.

Strakhov, V. N., 1991: Method of filtration for linear algebraic equations as a tool for solving linear problems of gravimetry and magnetometry (in Russian). *Dok. Acad. Nauk SSSR,* **3,** 595–599.

——, and G. M. Valyashko, 1981: Adaptive regularization of linear illposed problems (in Russian). *Dok. Acad. Nauk SSSR,* **267,** 546–548.

——, and A. B. Strakhov, 1999: Generalized least square and regularized solutions for the system of perturbed linear algebraic equations in geophysics. Part 1. *Geophys. J.,* **21,** 3–25.

Tikhonov, A. N., A. V. Goncharsky, V. V. Stepanov, and A. G. Yagola, 1995: *Numerical Methods for Solving Ill-Posed Problems.* Kluwer, 264 pp.

Vapnik, V. H., 1983: *Reconstruction of Empirical Laws from Observations* (in Russian). Nauka, 447 pp.

Vladimirov, V. S., 1971: *Equations of Mathematical Physics.* Deker, 357 pp.

Wahba, G., and J. Wendelberger, 1980: Some new mathematical methods for variational objective analysis using splines and cross validation. *Mon. Wea. Rev.,* **108,** 1122–1143.

Zeldovich, Y. B., A. A. Ruzmaikin, and V. V. Sokolov, 1985: Representation of a three-dimensional vector field by scalar potentials. *Sov. Phys. Dok.,* **30,** 756–758.